Experimental Seismic Behavior of a Full-Scale Four-Story Soft-Story Wood-Frame Building with Retrofits. II: Shake Table Test Results

John W. van de Lindt, F.ASCE[1]; Pouria Bahmani, A.M.ASCE[2]; Gary Mochizuki, M.ASCE[3]; Steven E. Pryor, M.ASCE[4]; Mikhail Gershfeld, M.ASCE[5]; Jingjing Tian, S.M.ASCE[6]; Michael D. Symans, M.ASCE[7]; and Douglas Rammer, M.ASCE[8]

Downloaded from ascelibrary.org by University of Wisconsin-Madison on 10/03/17. Copyright ASCE. For personal use only; all rights reserved.

Abstract: Soft-story wood-frame buildings have been recognized as a disaster preparedness problem for decades. The majority of these buildings were constructed from the 1920s to the 1960s and are prone to collapse during moderate to large earthquakes due to a characteristic deficiency in strength and stiffness in their first story. In order to propose and validate retrofit methods for these at-risk buildings, a full-scale four-story soft-story wood-frame building was constructed, retrofitted, and subjected to ground motions of various intensities. The tests were conducted to validate retrofit guidelines proposed in a "Federal Emergency Management Agency's recent soft-story seismic retrofit guideline for wood buildings" and a performance-based seismic retrofit (PBSR) methodology developed as part of the NEES-Soft project. This paper is the second in a set of companion papers and presents the full-scale shake table test results using the two new approaches. The companion paper to this paper presents the design philosophies, design details, and numerical analysis of the retrofitted building for each of the four retrofits. **DOI: 10.1061/(ASCE)ST.1943-541X.0001206.** © *2014 American Society of Civil Engineers.*

Author keywords: Soft-story; Wood frame; Shake table; Seismic retrofit; Seismic performance; FEMA P-807; Performance-based seismic retrofit; Wood structures.

Introduction

A number of full-scale tests on light-frame wood (wood-frame) buildings have been performed worldwide over the last several decades; however, none of the tests addressed the retrofit of soft-story buildings predominantly found in the San Francisco Bay Area. As part of the NEES–Soft project, a four-story soft-story wood-frame building was constructed, retrofitted, and tested on the largest shake table in the United States. A brief summary of the retrofit design is provided in this paper and details of the building design and numerical validations are presented in the companion paper (Bahmani et al. 2014). The focus of this paper is the shake table test results of the full-scale four-story wood-frame building with a soft and weak first story. Testing was conducted during the summer of 2013 at the NEES outdoor shake table at the University of California San Diego (UCSD). The comprehensive test program examined each of the four retrofits experimentally, namely, (1) cross-laminated timber (CLT) rocking walls based on a retrofit based on the FEMA P-807 (FEMA 2012) guidelines and a recent City of San Francisco soft-story retrofit ordinance, (2) steel special moment frames (SMFs) based on the FEMA P-807 retrofit guideline, (3) SMF and wood shear walls based on a performance-based seismic retrofit (PBSR) method developed as part of the NEES-Soft project (Bahmani et al. 2014), and (4) supplemental damper assemblies designed based on a PBSR methodology.

There were several major test objectives: (1) to experimentally determine whether the FEMA P-807 guideline is effective and should be recommended by the NEES-Soft project team for use to the practicing earthquake engineering community, (2) to determine whether the retrofits designed based on the PBSR methodology allowed the building to meet its performance objectives, (3) to provide a better understanding of the global behavior of full-scale soft-story wood-frame buildings, and (4) to gain better insight into the collapse limits of soft-story wood-frame buildings with archaic building materials. The full data set is archived on NEEShub and is available to the public at http://www.nees.org in perpetuity.

Description of Test Structure

In order to investigate the performance of soft-story buildings subjected to seismic ground motion, a four-story building with a soft story at its first story was designed and constructed on the shake table at the NEES-UCSD laboratory. Fig. 1 presents isometric views of the building from four directions. The building represented a

[1]George T. Abell Professor in Infrastructure, Dept. of Civil and Environmental Engineering, Colorado State Univ., Fort Collins, CO 80523-1372 (corresponding author). E-mail: jwv@engr.colostate.edu

[2]Ph.D. Candidate, Dept. of Civil and Environmental Engineering, Colorado State Univ., Fort Collins, CO 80523-1372. E-mail: pbahmani@engr.colostate.edu

[3]Senior Research and Development Engineer, Simpson Strong-Tie, Pleasanton, CA 94588.

[4]International Director of Building Systems, Simpson Strong-Tie, Pleasanton, CA 94588.

[5]Professional Practice Professor, Civil Engineering, Cal Poly, Pomona, CA 91768.

[6]Ph.D. Candidate, Civil and Environmental Engineering, Rensselaer Polytechnic Institute, Troy, NY 12180.

[7]Associate Professor, Civil and Environmental Engineering, Rensselaer Polytechnic Institute, Troy, NY 12180.

[8]Research Engineer, Forest Products Laboratory, Madison, WI 53726.

Note. This manuscript was submitted on May 29, 2014; approved on October 24, 2014; published online on December 9, 2014. Discussion period open until May 9, 2015; separate discussions must be submitted for individual papers. This paper is part of the ***Journal of Structural Engineering***, © ASCE, ISSN 0733-9445/E4014004(14)/$25.00.

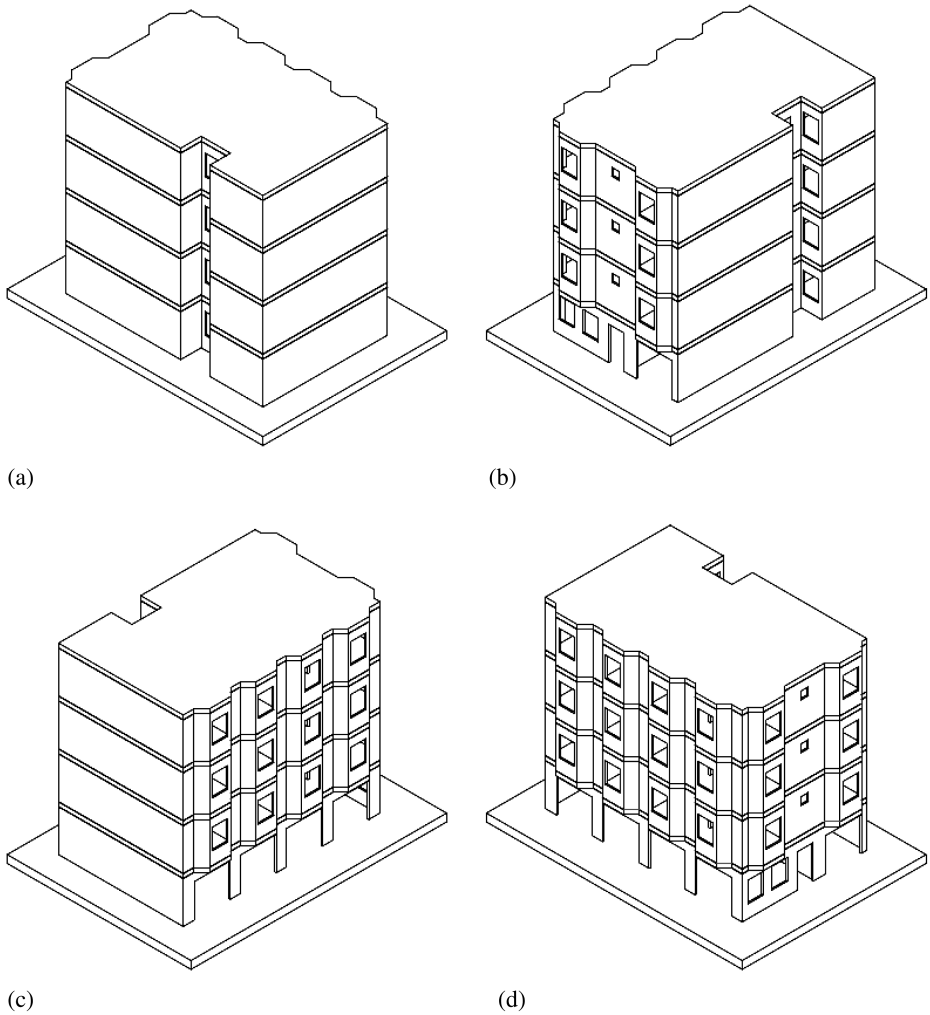

Fig. 1. Three-dimensional (3D) isometric views of the test building: (a) northwest view; (b) northeast view; (c) southwest view; (d) southeast view

corner building with two adjacent buildings on the north and west sides. The test building had four garage doors at the first story on its south side and two windows, a storage, and an entrance door on its east side. The upper stories each had two two-bedroom units with bay windows on the south and east sides. The details of the plan and elevation views of the building are presented in the companion paper (Bahmani et al. 2014). It can be seen that the large openings due to garage and storage doors reduce the available space for lateral load resisting systems, i.e., shear walls, thus, the building is soft and weak at the first floor.

As mentioned in the companion paper, the effectiveness of two retrofit methodologies (i.e., FEMA P-807 and PBSR) were examined experimentally during four testing phases in the summer of 2013 at the outdoor shake table facility NEES-UCSD. Cross-laminated timber and steel special moment frames were used to retrofit the building in accordance with the FEMA P-807 ordinance, and steel special moment frames, wood structural panels (WSPs), and fluid viscous dampers (FVDs) were used to retrofit the building using a PBSR methodology. The details of the retrofit design and location of the retrofit elements are presented in the companion paper (Bahmani et al. 2014) and Tian et al. (2014). The shake table is a 7.6×12.2 m $(25 \times 40$ ft$)$ uniaxial shake table with a maximum gravity payload of 20,000 kN (4,496 kips); full details on the shake table performance and capabilities can be found in Ozcelik et al. (2008).

Phase 1 (P-807 CLT)

Cross-laminated timber is a new sustainable wood product that has been used to build low- and mid-rise buildings in Europe and New Zealand and is just gaining traction in North America (Karacabeyli and Douglas 2013). These panels were used to retrofit the soft story (i.e., first story) of the test specimen using the FEMA P-807 retrofit procedures. Fig. 2(a) presents the location of CLT panels in the first story (marked by "CLT"). A total of seven 0.61-m-long (2-ft-long) panels were installed along the X- and Y-directions (three in the X-direction and four in the Y-direction) in order to add the required strength to the first story. The objective of the design was to limit the first story drift to 4% and reduce torsion based on the methodology of the FEMA P-807 guidelines for as high a seismic intensity as possible with only first-story retrofit, which in the case of the CLT rocking walls was 0.9 g spectral acceleration. Design details are presented in the companion paper (Bahmani et al. 2014).

Phase 2 (P-807 SMF)

For the second phase of testing, steel SMFs were used to retrofit the soft story (i.e., first story). The required strength and stiffness of the SMFs were again calculated based on the FEMA P-807 guideline, but the SMF retrofit was capable of achieving the requirements at 1.1 g spectral acceleration. A single one-bay SMF was installed in the X-direction (i.e., line D) and Y-direction (i.e., line 5) to

Downloaded from ascelibrary.org by University of Wisconsin-Madison on 10/03/17. Copyright ASCE. For personal use only; all rights reserved.

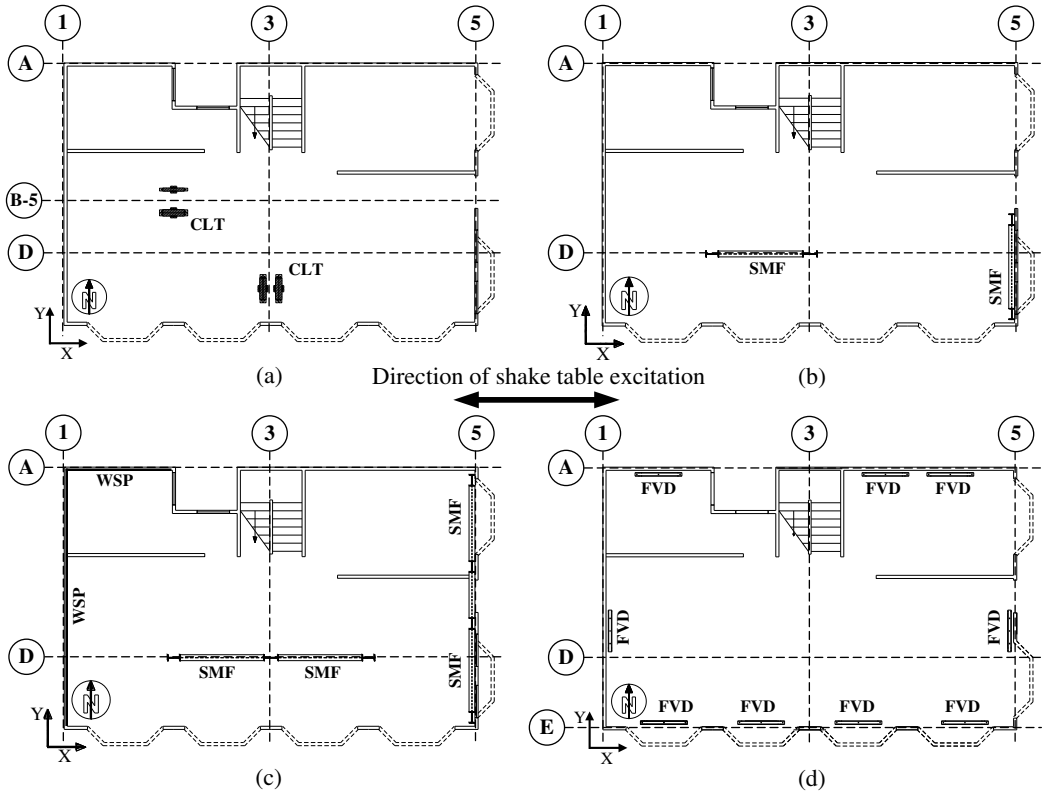

Fig. 2. Location of retrofit elements in the first story: (a) P-807 CLT; (b) P-807 SMF; (c) PBSR SMF; (d) PBSR FVD

strengthen the first story and also reduce the torsional response of the building. The locations of steel frames are presented in Fig. 2(b) and are marked by "SMF." The frames were installed such that they did not interfere with garage parking space in the first story. The wood structural panels on grid line A and grid line 1 were not installed in the test specimen. This was a construction oversight and was discovered just prior to conducting the test. Numerical analysis was performed to check if a delay was necessary and it was determined that the difference was negligible, i.e., less than 1% of the in-line response of the building.

Phase 3 (PBSR SMF)

In the third phase of testing, the building was retrofitted using the PBSR retrofit methodology developed as part of the project (Bahmani et al. 2014). In this method, the required stiffness and strength of the entire building are calculated using the performance-based seismic design (PBSD) methodology and additional stiffness and strength can be provided based on the desired retrofit techniques. In this third phase of testing, steel SMFs and WSPs were used to strengthen the building over the height and in the plane of each story to satisfy the performance criteria both for translation and rotation responses. The objective was to first eliminate torsion in the first story and then design the retrofit for a 2% story drift associated with a 50% nonexceedance at the maximum considered earthquake (MCE), which was 1.8 g spectral acceleration for a hypothetical site selected within the project. Continuous steel rods [i.e., anchor tie down system (ATS)] that react at each story sill plate were used to resist overturning and were installed at the ends of each wood shear wall. This is somewhat typical for multistory wood-frame buildings in high seismic regions of North America, but one additional performance constraint was imposed: the steel rods were sized such that elongation at ultimate demand during an MCE was limited to 6.4 mm (1/4 in.).

Fig. 2(c) presents the location of the SMF and WSP at the first story, marked "SMF" and "WSP," respectively. A two-bay steel SMF was installed along the X-direction (i.e., line D) and Y-direction (i.e., line 5) and was appropriately connected to the floor above to transfer the shear forces to the foundation. The connection between steel frame and wood floor was designed such that the shear force between these two elements could be transferred without any slippage between or damage to either of the elements. Due to the higher strength and stiffness of the steel moment frames than the stiffness of the existing wood walls, the center of rigidity in the first floor moved toward the SMF, which increased the eccentricity. In order to reduce the eccentricity at the first floor, wood structural panels were installed on the other side of the center of mass (CM) in the first story [i.e., lines A and 1 in Fig. 2(c)] to offset the effect of the SMFs on eccentricity.

The upper stories were retrofitted using WSPs. Fig. 3 presents the location of the WSPs at the upper stories. The location and stiffness of the WSPs were calculated such that the eccentricity at the upper stories was practically eliminated (close to zero), similar to the approach used for the first story. In general, the story shear decreases in the stories further away from ground. In order to distribute the required strength and stiffness in this building to the upper stories, different shear wall nail spacing was used in each story. Specifically, the same WSP length and panel thickness was used at each story (except on lines A and 3 at the fourth story), i.e., stacking the walls similar to a modern engineered wood building, and closer nail spacing was used for the lower stories to obtain higher strength and stiffness. ATS rods were used to transfer the uplift forces induced at each shear wall to the foundation. Again, for further details of the design and retrofit elements the interested reader is referred to the companion paper (Bahmani et al. 2014).

Downloaded from ascelibrary.org by University of Wisconsin-Madison on 10/03/17. Copyright ASCE. For personal use only; all rights reserved.

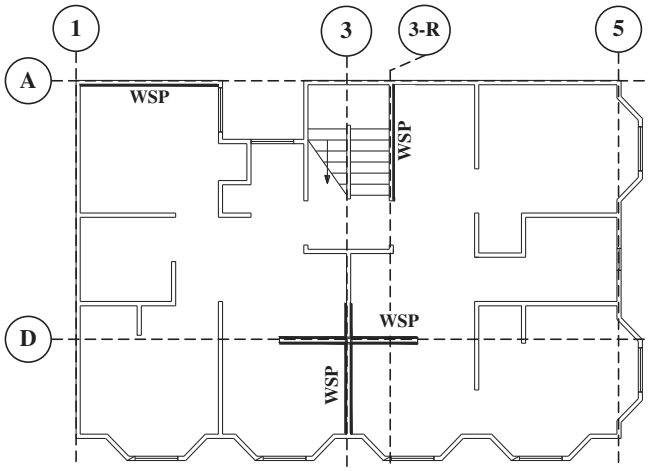

Fig. 3. Location of the WSPs on stories 2–4

Phase 4 (PBSR FVD)

In the last phase of retrofit testing, damper assemblies consisting of FVDs installed in toggle-braced frames were used to retrofit the first story of the test building. The damper assemblies provided a supplemental mechanism of dissipating seismically induced energy, thus reducing the energy dissipation demand on the lateral force resisting system (i.e., shear walls) within the structure. Seven dampers were installed along the X-direction and two dampers were installed along the Y-direction [Fig. 2(d) for location of damper assemblies in the first story]. The particular damper assemblies used in the testing were not specifically designed for this project, and thus to simplify installation, no effort was made to avoid placement in the garage door openings on the south wall line. Alternate damper assemblies that would be better suited for implementation in soft stories are presented in Schott et al. (2014). The damper assemblies were strategically distributed in the first story to achieve a near-optimized structural behavior (Tian and Symans 2012). The upper stories were retrofitted with WSPs at selected locations and with various wall lengths and nail patterns as presented in the Phase 3 discussion. In comparison to the WSP in Phase 3, the WSP in the first story (along wall lines 1 and A) was removed based on the PBSR for the FVD. Because the design of the upper-story retrofits was conducted specifically for the stiffening and strengthening type of retrofit utilized in Phase 3 (which was conducted prior to Phase 4 and thus was in place for the Phase 4 testing), it does not necessarily represent an optimal retrofit solution for Phase 4 wherein a supplemental damper retrofit was incorporated. The details of the PBSR FVD retrofit design can be found in Tian et al. (2014). The building was subjected to uniaxial excitation along its longitudinal direction (i.e., X-direction) because the shake table at the NEES at UCSD facility is uniaxial.

Instrumentation

The responses of the building to seismic excitation were recorded by approximately 400 sensors that were installed in different locations throughout the building. Two accelerometers were installed at every corner of each story and at the CM of each floor diaphragm to record the acceleration in both the X- and Y-directions. Two arrays of five accelerometers were installed at each of the two-bedroom units to record the accelerations and eventually to compute displacement (via numerical integration over time) of the diaphragm during each seismic test. String potentiometers and linear potentiometers were installed in different locations to record the displacement of shear walls due to shear and uplift forces. Strain gauges were installed on the steel special moment frame and ATS rods to record the strains at different locations of the frames and elongation on the ATS rods. Twenty-two load cells were installed underneath the anchor bolts of the exterior and interior walls of the first story to record the uplift forces at each anchor bolt. Fig. 4 presents typical locations of accelerometers and string potentiometers within the first story and Table 1 presents the type, location, and quantity of each sensor used in the tests.

Ground Motion Records

In order to verify the effectiveness of the retrofits under seismic loading, the building was subjected to two different ground motions. The 1989 Loma Prieta-Gilroy (component G03000) earthquake record and the 1992 Cape Mendocino-Rio (component RIO360) earthquake record were selected and scaled to different spectral accelerations for each phase of testing. Table 2 presents the ground motions and their corresponding peak ground accelerations (PGAs) and spectral accelerations for each phase of the test program. Figs. 5(a and b) present the spectral acceleration for the

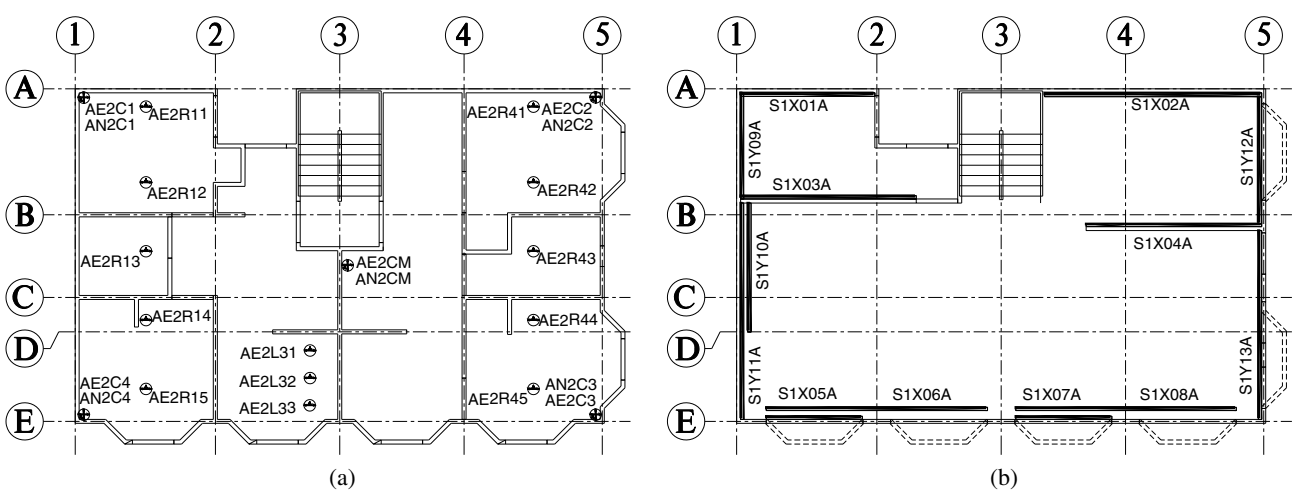

Fig. 4. Location of sensors installed in the first story: (a) accelerometers; (b) string potentiometers

Downloaded from ascelibrary.org by University of Wisconsin-Madison on 10/03/17. Copyright ASCE. For personal use only; all rights reserved.

Table 1. Summary of Instrumentation for Each Testing Phase of NEES-Soft Project

Measurement	Location	Sensor type	Quantity for each phase			
			1	2	3	4
Absolute acceleration[a]	Each floor	Accelerometer	91	91	91	90
Anchor bolt force	First floor	Load cell	22	22	22	22
Floor displacement[b]	Building exterior	String potentiometer	8	8	8	8
In-plane diaphragm deformation	Bedrooms	String potentiometer	12	12	12	12
Shear wall diagonal deformation	Selected shear wall	String potentiometer	59	55	51	54
Shear wall slippage and uplift	Selected shear wall	Linear potentiometer	86	86	50	47
ATS hold-down strain	ATS rods	Strain gauge	—	—	60	60
Strain on threaded rods on CLT	Threaded rods	Strain gauge	32	—	—	—
CLT uplift and slippage	CLT panels	Linear potentiometer	8	—	—	—
SMF lateral deformation	SMF frames	Linear potentiometer	—	2	2	—
Strain on SMF	SMF column, beam, link	Strain gauge	—	32	95	—
SMF base rotation and uplift	SMF base connection	Linear potentiometer	—	—	5	—
FVD axial deformation	Damper frame	Linear potentiometer	—	—	—	9
FVD frame diagonal deformation	Damper frame	String potentiometer	—	—	—	9
FVD frame slippage/uplift	Damper frame connection	Linear potentiometer	—	—	—	22
Total			318	308	396	333

[a]Two-dimensional (2D) accelerometer at the corners and center of mass of each floor.
[b]Diagonal string potentiometers installed at west and north side of the building from base steel to each floor.

Table 2. Test Sequences and Global Response for Each Testing Phase

Phase	Seismic test[a]	S_a (g)	PGA (g)	Earthquake[b]	Average peak interstory drift ratio[c,d] (%)				Normalized maximum story shear ($C_i = V_i/W$)[e]			
					Story 1	Story 2	Story 3	Story 4	Story 1	Story 2	Story 3	Story 4
P807 CLT	1	0.20	0.11	LP	0.20	0.06	0.07	0.04	0.11	0.10	0.07	0.03
	2	0.20	0.10	RIO	0.24	0.09	0.08	0.04	0.13	0.11	0.08	0.03
	3	0.90	0.49	LP	1.43	0.32	0.33	0.23	0.28	0.26	0.20	0.10
	4	0.90	0.45	RIO	1.54	0.35	0.36	0.24	0.28	0.26	0.19	0.09
P807 SMF	5	0.24	0.13	LP	0.27	0.11	0.11	0.05	0.10	0.09	0.07	0.03
	6	0.24	0.12	RIO	0.38	0.13	0.14	0.06	0.13	0.11	0.08	0.04
	7	1.10	0.60	LP	1.95	0.40	0.42	0.27	0.30	0.27	0.23	0.12
	8	1.10	0.55	RIO	1.66	0.46	0.47	0.27	0.31	0.29	0.22	0.11
PBSR SMF	9	0.20	0.11	LP	0.14	0.12	0.11	0.04	0.14	0.12	0.09	0.04
	10	1.20	0.65	LP	1.05	0.99	1.07	0.25	0.54	0.52	0.44	0.22
	11	1.20	0.60	RIO	0.97	1.38	1.48	0.25	0.54	0.56	0.47	0.24
	12	1.80	0.90	RIO	1.05	1.83	2.26	0.43	0.54	0.63	0.54	0.29
	13	1.80	0.98	LP	1.35	1.55	1.94	0.40	0.60	0.54	0.48	0.27
PBSR FVD	14	0.50	0.27	LP	0.23	0.34	0.50	0.08	0.14	0.12	0.12	0.06
	15	1.20	0.65	LP	0.67	0.77	1.11	0.19	0.32	0.25	0.26	0.17
	16	1.20	0.60	RIO	0.52	1.03	1.44	0.28	0.25	0.29	0.32	0.19
	17	1.80	0.98	LP	1.07	1.11	1.60	0.37	0.44	0.35	0.41	0.26
	18	1.80	0.90	RIO	1.07	1.11	1.60	0.37	0.36	0.41	0.44	0.27

[a]Only seismic test numbers are shown; white noise tests of 0.05 g RMS were conducted between all tests and/or repairs (Fig. 6).
[b]LP and RIO refer to Loma Prieta-Gilroy and Cape Mendocino-Rio earthquake ground motions, respectively.
[c]Average of drifts recorded at four corners of the building at each story.
[d]Effective height of 2,438 mm (96 in.) was used in calculating interstory drift ratios.
[e]Total weight of the building above the base steel, $W = 467$ kN (105 kips); V_i is the story shear.

two ground motions scaled to $S_a = 1.2$ g and $S_a = 1.8$ g, respectively, and the acceleration time histories of the ground motions scaled to the MCE level (i.e., $S_a = 1.8$ g) are presented in Figs. 5 (c and d). For scaling the ground motions, 22 biaxial far-field earthquake ground motion records of FEMA P-695 (FEMA 2009) were used. Each ground motion consisted of a pair of horizontal ground motions in the X- and Y-directions. A square root of the sum of the squares (SRSS) spectrum was constructed by taking the SRSS of the 5%-damped response spectra of two components of each pair of the horizontal ground motion components. Each pair of ground motions was scaled such that in the period range from 0.08 to 1.5 s, the average of the SRSS spectra of all pairs of components did not fall below the site design spectrum. This period range represented 0.2 times the period of the stiffest retrofitted building to 1.5 times the period of the unretrofitted building based on the numerically predicted periods. For generation of the design spectrum in the San Francisco Bay Area, the spectral response acceleration at short periods (S_s) and at a period of 1.0 s (S_1) were 1.8 and 1.2 g, respectively. The building was retrofitted in both the X- and Y-directions to withstand biaxial ground motions and satisfy the performance criteria (i.e., translational and torsional responses); therefore, the biaxial ground motion scaling procedure consistent with ASCE 7-10 (ASCE 2010) was used even though the shake table was able to produce excitation in the X-direction only.

Downloaded from ascelibrary.org by University of Wisconsin-Madison on 10/03/17. Copyright ASCE. For personal use only; all rights reserved.

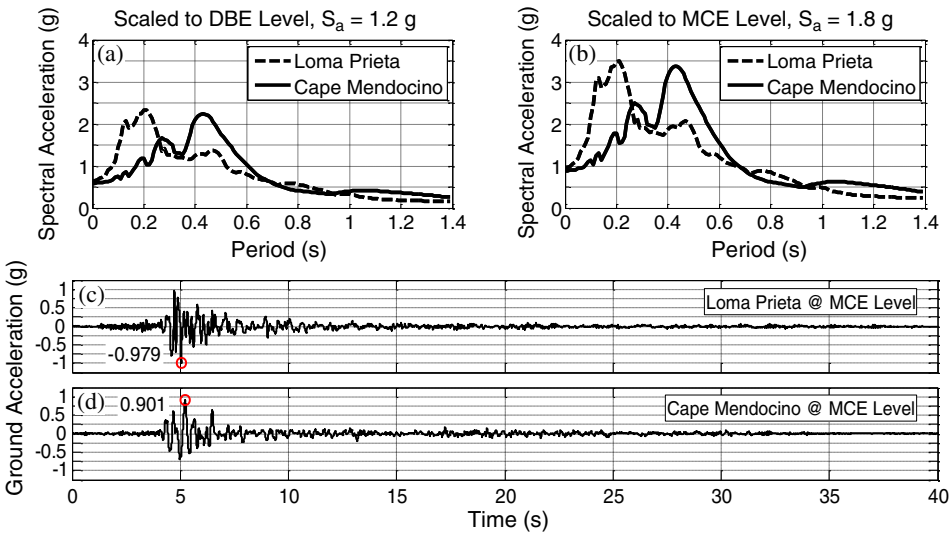

Fig. 5. Ground motions and spectral accelerations: (a) spectral acceleration scaled to 1.2 g; (b) spectral acceleration scaled to 1.8 g; (c) Loma Prieta record scaled to $S_a = 1.8$ g; (d) Cape Mendocino record scaled to $S_a = 1.8$ g

Fundamental Period and Repair

In order to obtain the natural frequencies of the test building prior to and after each seismic test a white noise test with an RMS acceleration amplitude of 0.05 g was conducted. Generally, after each seismic test the fundamental period of the building increased due to structural and nonstructural damage. Following repairs to the first story of the building, the fundamental period of the building decreased to approach the initial fundamental period of the test building at the undamaged state. Fig. 6 presents the fundamental period of the building tracked during all four testing phases. The fundamental period of the building without any retrofit (i.e., the original condition) was approximately 1.0 s. The initial fundamental period of the building before Phases 1 and 2 was 0.58 s and before Phases 3 and 4 was 0.41 and 0.55 s, respectively. During Phases 3 and 4, the building was subjected to MCE-level earthquakes with spectral acceleration of 1.8 g that ultimately increased the overall fundamental period of the building even after repairing the building. This most likely occurred as the horizontal wood siding (HWS), which was fastened with two nails forming a moment couple, racked, and loosened slightly during strong shakes. During each repair and damage inspection, additional drywall screws were added to the drywall with loose connectors and withdrawn nails in HWSs and WSPs were replaced. Some drywalls were also replaced due to observation of shear cracks and significant lack of transferring shear force.

Global Responses

As mentioned previously, the four-story test building was retrofitted using four different retrofit techniques and was subjected to Loma Prieta-Gilroy and Cape Mendocino-Rio ground motions.

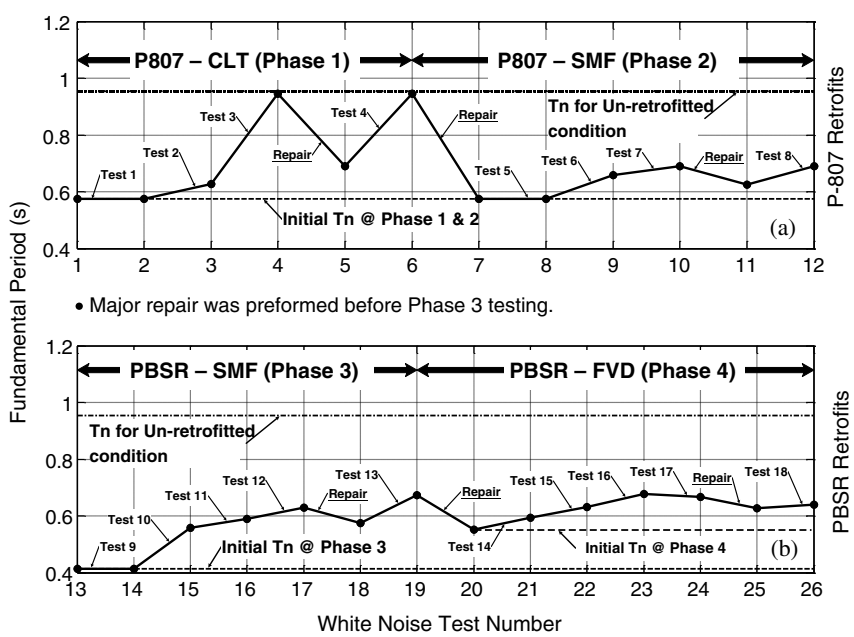

Fig. 6. Fundamental period of the building and effect of repair for each testing phase: (a) P-807 retrofits; (b) PBSR retrofits

Downloaded from ascelibrary.org by University of Wisconsin-Madison on 10/03/17. Copyright ASCE. For personal use only; all rights reserved.

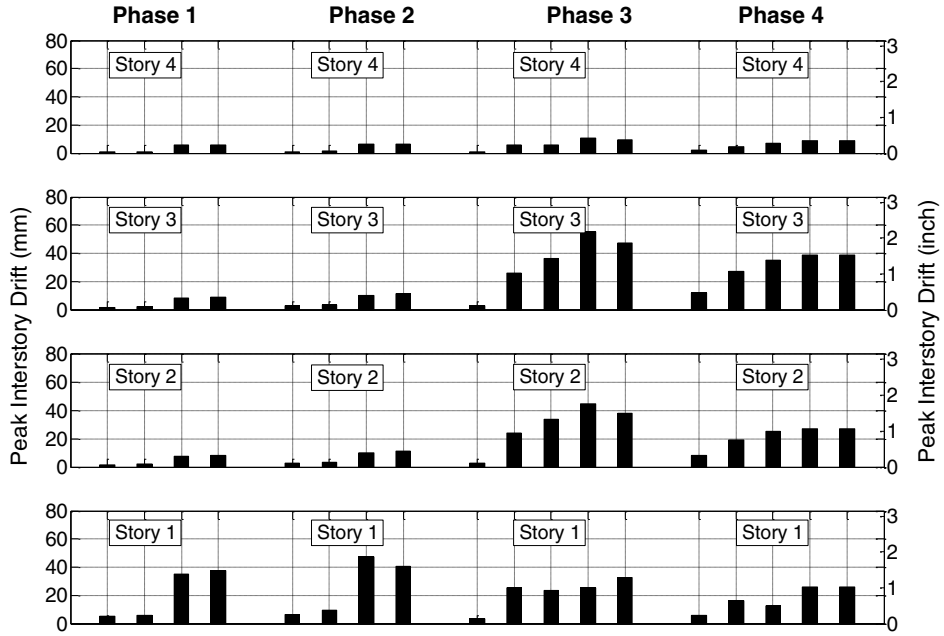

Test ID	1	2	3	4	5	6	7	8	9	10	11	12	13	14	15	16	17	18
PGA (g)	0.11	0.10	0.49	0.45	0.13	0.12	0.60	0.55	0.11	0.65	0.60	0.90	0.98	0.27	0.65	0.60	0.98	0.90
Sa (g)	0.20	0.20	0.90	0.90	0.24	0.24	1.10	1.10	0.20	1.20	1.20	1.80	1.80	0.50	1.20	1.20	1.80	1.80

Fig. 7. Peak interstory drifts (ISDs) for each seismic test

Peak Interstory Drifts

The maximum interstory drifts (ISDs) in the X-direction (i.e., parallel to the direction of shake table motion) were obtained by taking the average of the accelerations recorded at the corner of each story. The average acceleration was integrated twice with respect to time to obtain absolute displacements. The average peak interstory drift ratios for all the seismic tests are presented in Table 2. Fig. 7 presents the average peak interstory drifts over the height of the building. The proper interpretation of the results in Table 2 and Fig. 7, as well as results that are presented in subsequent tables and figures, requires recognition that the seismic intensity for the PBSR retrofits was considerably larger than those for the FEMA P-807 retrofits (see spectral acceleration column Table 2 and the spectral acceleration values at the bottom of Fig. 7). It can be seen from the bar chart that the peak interstory drift occurs at the first story for the first two testing phases (the only story that was retrofitted per the FEMA P-807 guidelines). This is typical of a soft-story building response where the upper stories behave essentially as a rigid body and thus experience little damage. No structural or nonstructural damage was found in the upper stories during these first two phases with exception of minor hairline cracks near door and window corners on the second level. However, in Phases 3 and 4 in which a PBSR methodology was used to retrofit the building, all stories (except the fourth story) experienced interstory drifts of greater than approximately 25 mm (approximately 1 in.), emphasizing the fact that in the PBSR methodology the entire building should be designed such that all the stories would experience approximately the same interstory drifts. By distributing seismic demand over the height of the building, the building can resist ground excitations with much higher intensities. The basic idea is similar to fundamental inelastic earthquake engineering concepts (Chopra 2005) in which the objective is to distribute the seismic demand evenly throughout all the stories rather than have it concentrated in one story. Strengthening the building and increasing its stiffness decreases the natural period of the building resulting in higher spectral accelerations and correspondingly higher seismic forces at the foundation.

Building Displacement Profile

Fig. 8 presents the displacement profile of the test building for each phase of testing when the maximum displacement relative to the ground occurs at the roof level. Peak interstory drift of single stories does not necessarily occur when the roof is at its peak displacement, i.e., this would only occur in a first mode response. This was particularly noticeable during Phases 3 and 4 when a higher mode response was observed. It can be seen from Figs. 8(a and b) that the first story experienced the maximum interstory drift among all stories for the retrofits designed in accordance with the FEMA P-807 guidelines; the interstory drifts of the first story were kept less than the drift limit defined by the FEMA P-807 document (Bahmani et al. 2014).

Figs. 8(c and d) present the displacement profile of the building for Phases 3 and 4, respectively. It can be seen that all stories (except the fourth story) experienced interstory drifts such that the profile of the building is closer to a straight line (i.e., one of the basic assumptions in the PBSR methodology is that the stories are designed to achieve approximately the same peak drifts). However, the fourth story experienced lower ISD because the stiffness of the existing building at the fourth story was very close to the stiffness required according to the PBSR method. Namely, the fourth story was strengthened with WSPs that were needed to reduce the eccentricity in this story. Fig. 8(c) shows the profile of the building retrofitted with SMF and WSP subjected to the Loma Prieta and Cape Mendocino ground motions scaled to spectral accelerations ranging from $S_a = 0.2$ to 1.8 g. The maximum displacement of the roof occurred when the building was subjected to the Cape Mendocino ground motion

Downloaded from ascelibrary.org by University of Wisconsin-Madison on 10/03/17. Copyright ASCE. For personal use only; all rights reserved.

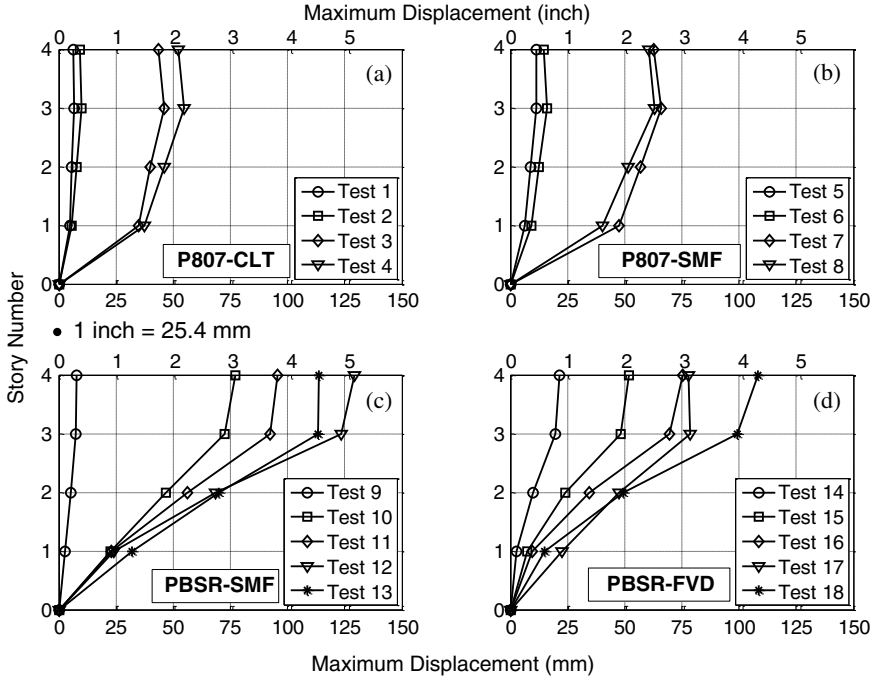

Fig. 8. Building displacement profile in X-direction: (a) Phase 1; (b) Phase 2; (c) Phase 3; (d) Phase 4

scaled to the MCE level. The maximum roof displacement relative to the ground was approximately 130 mm (approximately 5 in.).

Fig. 8(d) presents the profile of the building retrofitted with supplemental damper assemblies (i.e., FVD frame) in the first story and WSP in the upper stories. The building was subjected to ground motions scaled to spectral accelerations ranging from 0.5 to 1.8 g. The maximum roof displacement was approximately 110 mm (approximately 4.4 in.) under the Cape Mendocino ground motion scaled to the MCE level.

Global Hysteresis

The inertial force at each floor diaphragm was calculated by applying Newton's second law by using the spatial average of the acceleration time histories recorded at each corner of stories and the mass associated with each story. The shear force at each story was then calculated for all seismic tests. Table 2 presents the maximum story shear normalized by the weight of the building ($W = 467$ kN $= 105$ kips) for each seismic test. It can be seen that the maximum base shear coefficient, $C = V_{\text{Story}}/W$, was 0.60, which occurred during the last test of Phase 3 (Test 13). Fig. 9

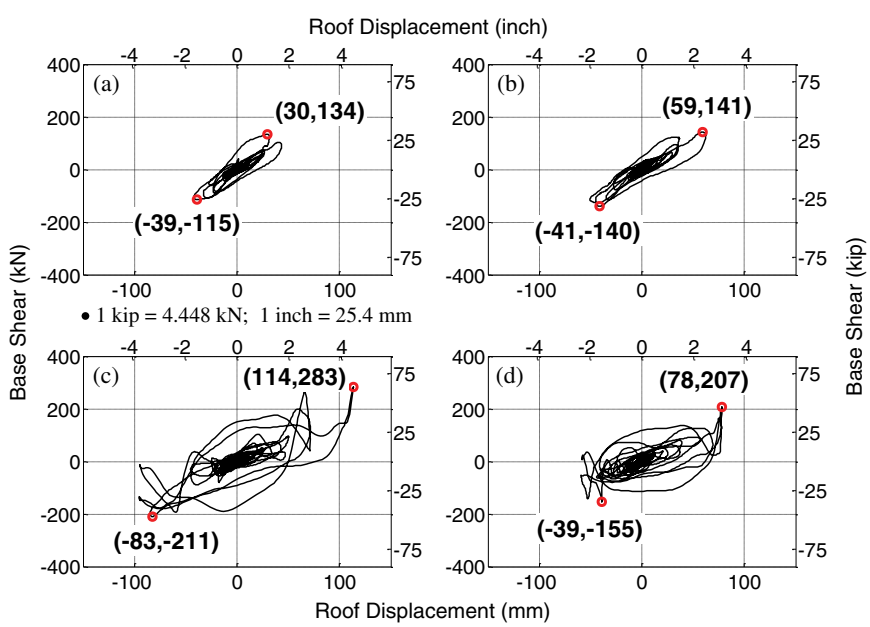

Fig. 9. Global hysteresis curves in the X-direction for the building subjected to Loma Prieta ground motion: (a) Phase 1, Test 3; (b) Phase 2, Test 7; (c) Phase 3, Test 13; (d) Phase 4, Test 17

Downloaded from ascelibrary.org by University of Wisconsin-Madison on 10/03/17. Copyright ASCE. For personal use only; all rights reserved.

presents the roof displacement versus the shear force at the base of the building (i.e., base shear) for the case of the Loma Prieta ground motion scaled to the maximum spectral acceleration for each test phase (i.e., $S_a = 0.9$ g for Phase 1, $S_a = 1.1$ g for Phase 2, and $S_a = 1.8$ g for Phases 3 and 4). It can be seen that the global hysteresis curves are smoother for the first two phases wherein the FEMA P-807 methodology was used to retrofit the building (the PBSR retrofits, Phases 3 and 4, are not as smooth). This behavior was expected because the FEMA P-807 retrofit tends to concentrate deformational response in the first (soft) story, thereby limiting the contribution of higher modes. However, as discussed previously, for the PBSR retrofit cases the higher modes had more effect on the response of the building, resulting in more complex global hysteretic behavior. The response of the building to the Loma Prieta ground motion is presented herein because this ground motion produced the highest base shears for all phases except Phase 2 (the base shear coefficient was 0.31 for Cape Mendocino and 0.30 for Loma Prieta in Phase 2).

Time-History Response

The responses to the Cape Mendocino-Rio record produced the maximum displacement profile of the building for all phases except Phase 2 (the displacement profiles for Tests 7 and 8 were close, but the response to Cape Mendocino was selected to be consistent in evaluating the results).

FEMA P-807 Retrofit

Figs. 10 and 11 present the translational response (interstory drift time histories) of the first and third stories of the building in both the X- and Y-directions for Phases 1 and 2, respectively. Figs. 10(a and b) and 11(a and b) present the average translational responses in the X-direction (i.e., parallel to the motion of the shake table) during Cape Mendocino-Rio ground motion scaled to $S_a = 0.9$ g for the building retrofitted with CLT panels and $S_a = 1.1$ g for the building retrofitted with SMF, respectively. It can be seen that the interstory drift recorded at the first story is approximately four times the interstory drift recorded at the third story. Thus, the first story is still soft even though it has been retrofitted, the result being more damage in the first story than in the upper stories (the upper stories only had hairline cracks in the drywall). Figs. 10(c and d) and 11(c and d) present the average translational response of the first and third stories in the Y-direction (perpendicular to the direction of shake table motion). It can be seen that the response of the building in this direction was very small, thereby demonstrating that torsion response had been effectively eliminated.

PBSR Retrofit

Figs. 12 and 13 present the translational time-history responses of the first and third stories of the building in both the X- and Y-directions for Phases 3 and 4, respectively. Figs. 12(a and b) and 13(a and b) present the average translational responses in the X-direction during the Cape Mendocino-Rio ground motion scaled

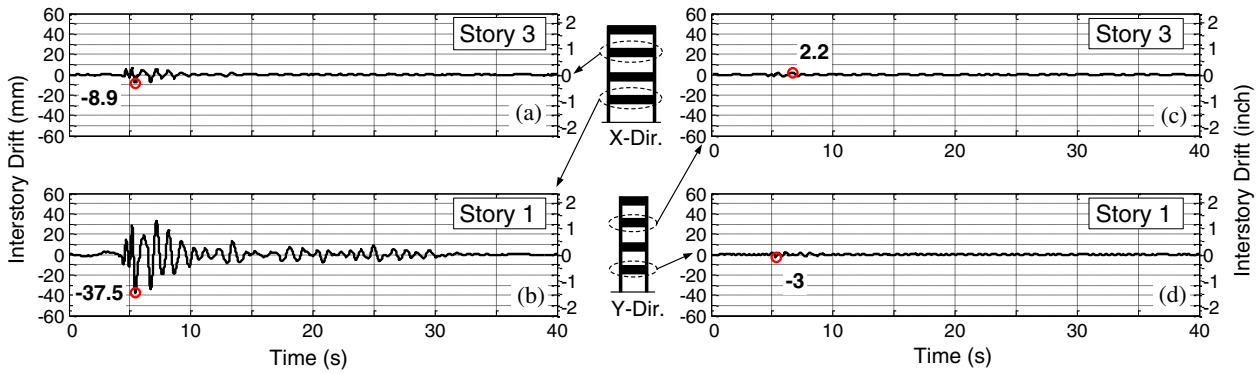

Fig. 10. Translational response of the building retrofitted with CLT panels and subjected to Cape Mendocino-Rio ground motion with PGA = 0.45 g: (a) X-direction, Story 3; (b) X-direction, Story 1; (c) Y-direction, Story 3; (d) Y-direction, Story 1

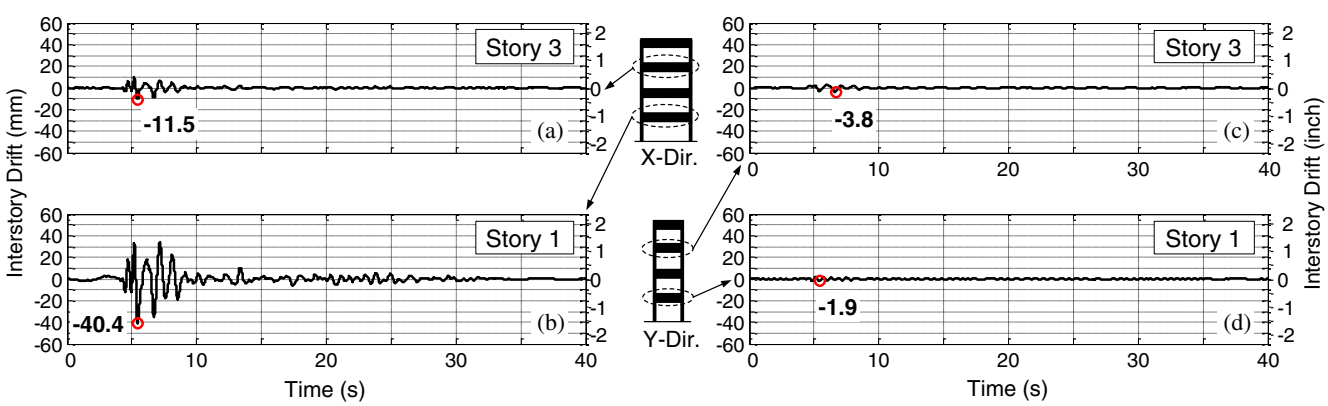

Fig. 11. Translational response of the building retrofitted with SMF and subjected to Cape Mendocino-Rio ground motion with PGA = 0.55 g: (a) X-direction, Story 3; (b) X-direction, Story 1; (c) Y-direction, Story 3; (d) Y-direction, Story 1

Downloaded from ascelibrary.org by University of Wisconsin-Madison on 10/03/17. Copyright ASCE. For personal use only; all rights reserved.

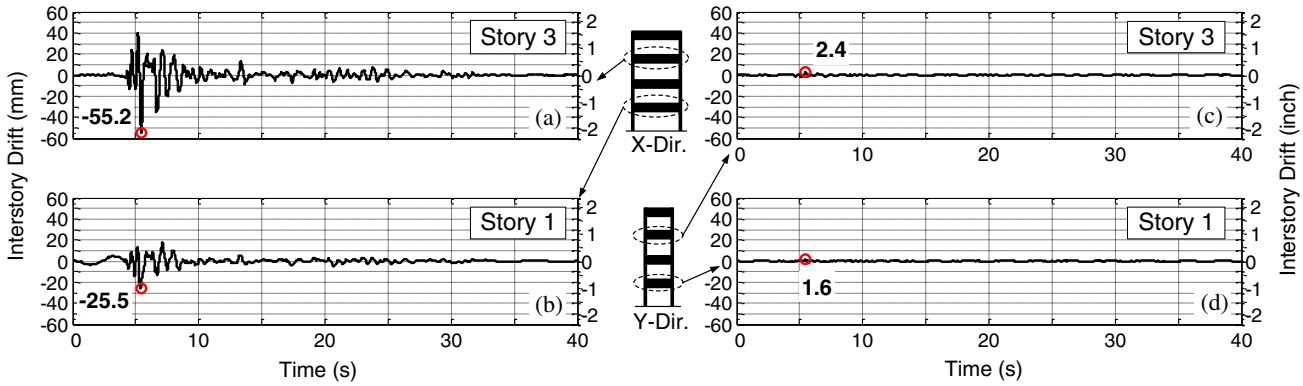

Fig. 12. Translational response of the building retrofitted with SMF and WSP and subjected to Cape Mendocino-Rio ground motion with PGA = 0.90 g: (a) X-direction, Story 3; (b) X-direction, Story 1; (c) Y-direction, Story 3; (d) Y-direction, Story 1

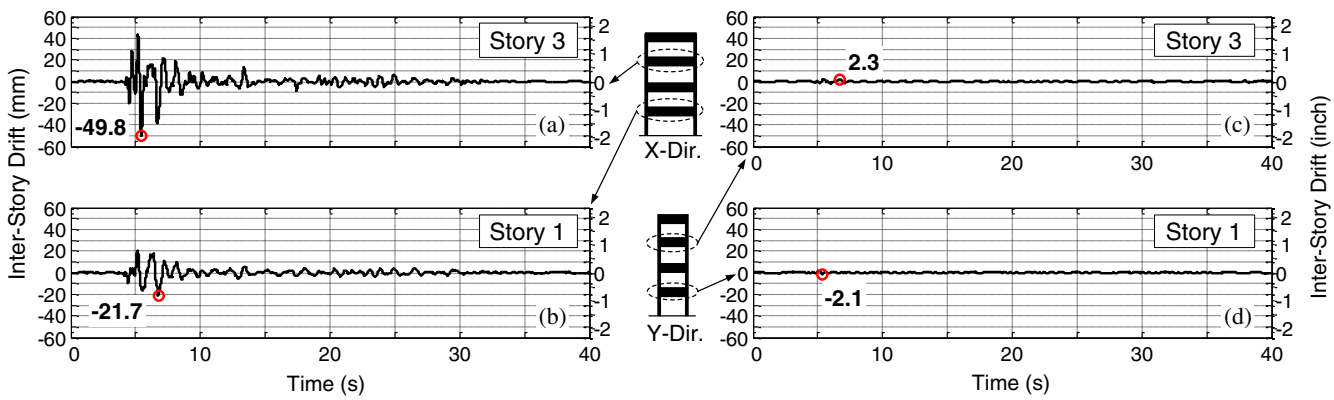

Fig. 13. Translational response of the building retrofitted with FVD and WSP and subjected to Cape Mendocino-Rio ground motion with PGA = 0.90 g: (a) X-direction, Story 3; (b) X-direction, Story 1; (c) Y-direction, Story 3; (d) Y-direction, Story 1

to $S_a = 1.8$ g for the building retrofitted with steel SMFs + WSPs and FVDs + WSP, respectively. It can be seen that the interstory drift recorded at the first story is approximately 25 mm (1 in.) and the peak interstory drift occurred at the third story. Figs. 12(c and d) and 13(c and d) present the average translational response of the first and third stories in the Y-direction. The peak response of the building perpendicular to the motion of the shake table was approximately 5 and 10% of the peak response in the X-direction for Phases 3 and 4 testing, respectively. Again, this shows that the torsional response of the building was essentially eliminated in these test phases.

Torsional Response

As mentioned previously, soft-story buildings can be soft in both translation and torsion. The four-story test building was not only soft in both translational directions, but also had a very low torsional stiffness due to high stiffness irregularity in the first story (e.g., location of garage doors, window openings). Both the FEMA P-807 guideline and PBSR retrofit methodology, discussed in this paper and the companion paper, are intended to eliminate torsional response of buildings by reducing eccentricities. The torsional responses of the test building at the roof level when subjected to the Cape Mendocino-Rio ground motion are shown in Fig. 14 for all phases. It can be seen that the rotational response of the building at roof level relative to the ground was 0.002 rad (0.11°) for the first two phases (FEMA P-807 retrofit) and 0.004 and 0.003 rad (0.23 and 0.17°) for Phases 3 and 4, respectively. Recall that the seismic intensity levels varied from Phase 1 to Phase 4.

Retrofit Component Response

The retrofit elements (e.g., CLT rocking walls, SMF, WSP, FVD) were monitored during each seismic test to ensure that they were engaging and to quantify their response to ground excitation for comparison and calibration with numerical models. Two retrofit elements were selected from the PBSR retrofits (Phase 3 and 4 tests) for presentation in this paper. Fig. 15 presents the plan view of the first story with the locations of the retrofit elements. The selected retrofit elements are circled with dashed lines. The displacement time-history responses of the SMF located at line D [Fig. 15(a)] were obtained using the accelerometers installed above the steel frame, then the displacement was applied as input to the bilinear spring model used in the design to obtain the lateral resisting force developed by the SMF. The same basic procedure was used to obtain the force in the damper frame (i.e., FVD) in line E except the displacement was obtained from a string potentiometer attached to the damper framing assembly and the displacement was applied as input to the viscous damper model used in the design to obtain the lateral resisting force developed by the damper framing assembly. Figs. 16 and 17 present the hysteresis curve (lateral force versus lateral displacement) and horizontal force

Downloaded from ascelibrary.org by University of Wisconsin-Madison on 10/03/17. Copyright ASCE. For personal use only; all rights reserved.

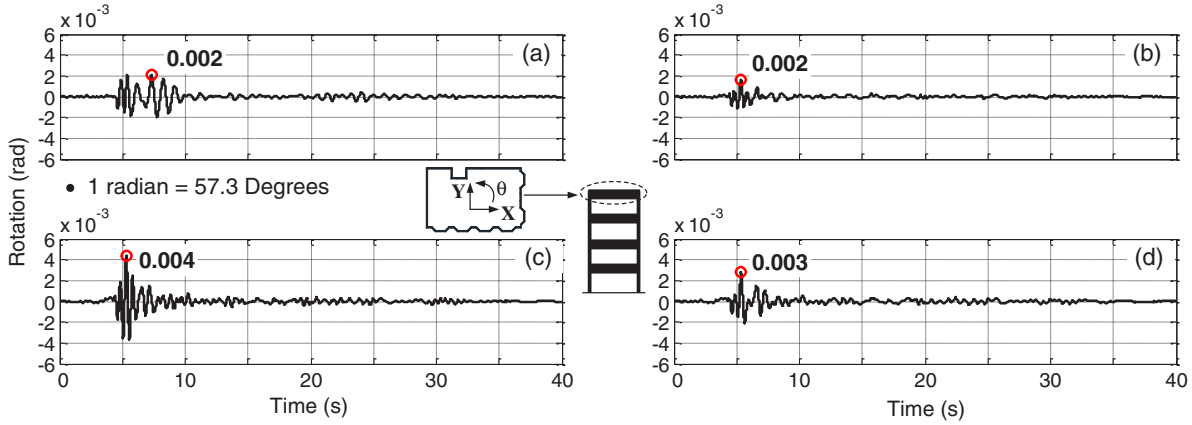

Fig. 14. Rotational response of the building measured at the roof level for Cape Mendocino ground motion: (a) Phase 1, PGA = 0.45 g; (b) Phase 2, PGA = 0.55 g; (c) Phase 3, PGA = 0.90 g; (d) Phase 4, PGA = 0.90 g

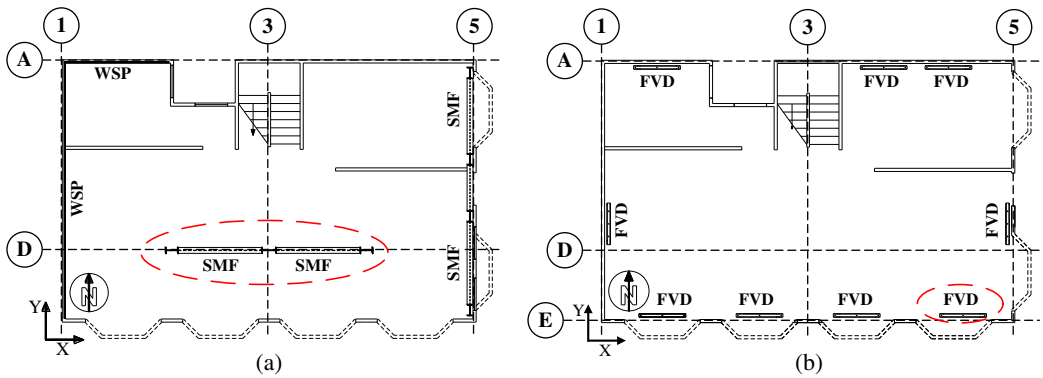

Fig. 15. Location of retrofit components in the *X*-direction: (a) Phase 3: steel SMF; (b) Phase 4: FVD frame

time-history responses of the selected SMF and damper assembly (i.e., FVD), respectively. The maximum lateral force occurred at the maximum lateral displacement for the SMF frame because the force and displacement were in phase, whereas the maximum lateral force of the damper assembly occurs at approximately zero displacement, which is due to the rate-dependent feature of FVDs (the generated force is proportional to the velocity).

Uplift Forces

As mentioned previously, ATS rods were installed adjacent to the end posts of each WSP for the PBSR retrofits to transfer the uplift forces at the end of shear walls down to the foundation (i.e., shake table). The location of the ATS rods at the first story and upper stories are shown in Fig. 18. A total of eight continuous ATS rods

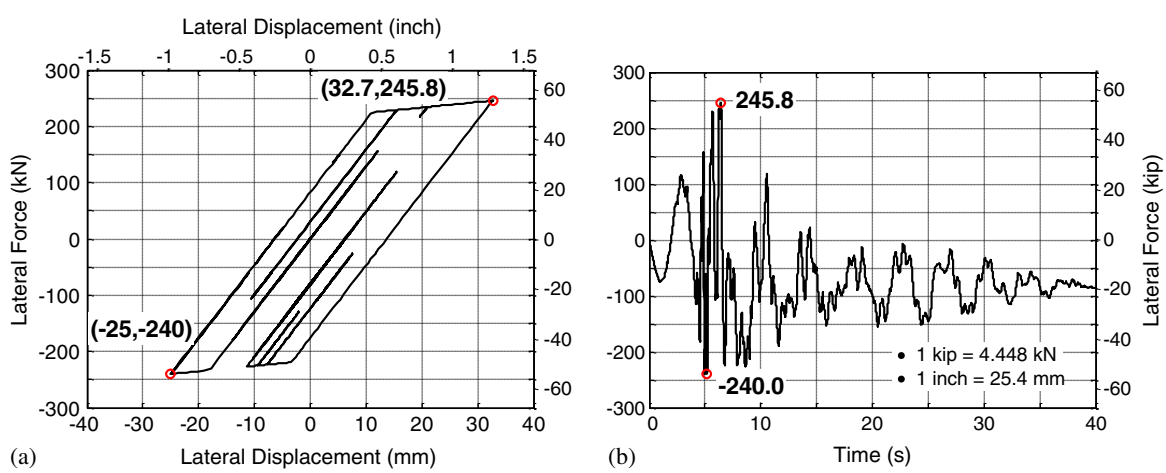

Fig. 16. Response of SMF frame located at the first floor along the *X*-direction for building subjected to Loma Prieta ground motion at the MCE level: (a) hysteresis curve; (b) force time-history response

Downloaded from ascelibrary.org by University of Wisconsin-Madison on 10/03/17. Copyright ASCE. For personal use only; all rights reserved.

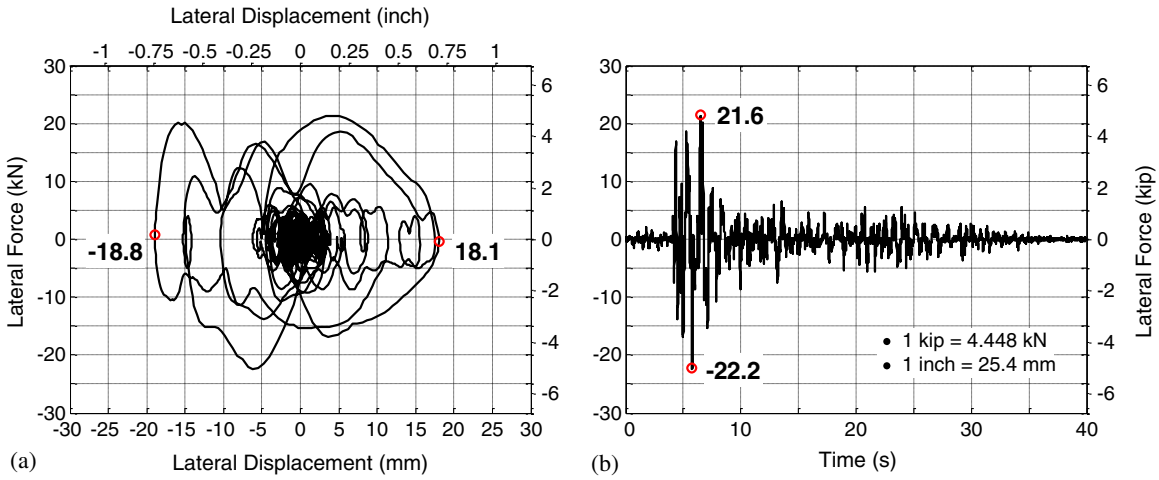

Fig. 17. Response of damper framing assembly (i.e., FVD) located at southeast corner of first story in the X-direction for building subjected to Cape Mendocino-Rio ground motion at MCE level: (a) hysteresis curve; (b) force time-history response

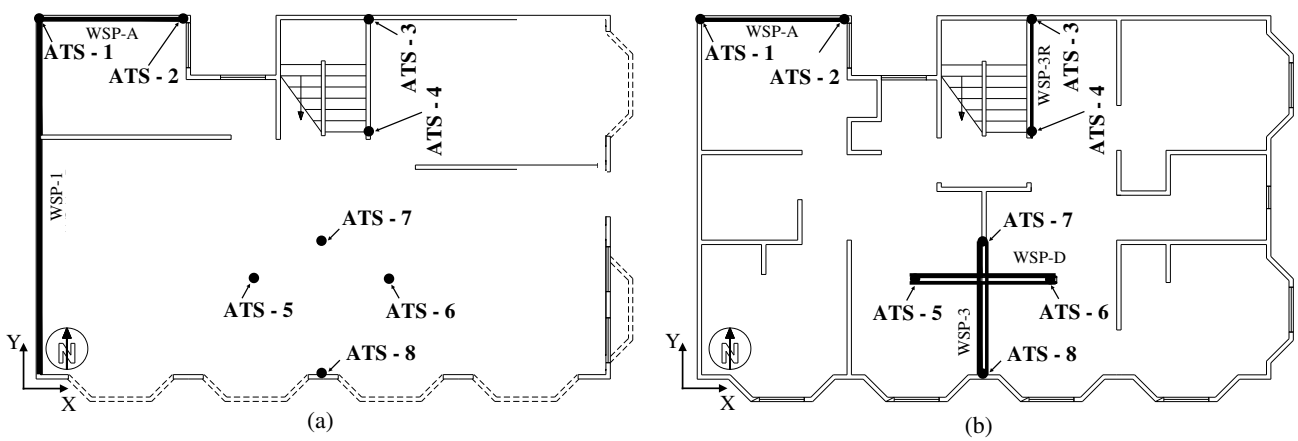

Fig. 18. Location of ATS rods: (a) first story; (b) upper stories

were installed in the test building. The required cross-sectional area of the rods was determined based on the maximum allowable uplift displacement in the rods and shear forces at each story. Details of the installation of ATS rods and cross-sectional areas for each rod are provided in the companion paper (Bahmani et al. 2014). The ATS rods are ideally located such that they do not interfere with garage parking spaces and the architectural aspects of the building. This was one of the most important factors in locating the WSPs for the upper stories.

Table 3 presents the maximum uplift force that occurred in the ATS rods when the test building was subjected to the Cape Mendocino-Rio ground motion at the MCE level. This record is presented herein because it resulted in the largest forces experienced by the rods during the entire test program. In Phase 3 (i.e., PBSR SMF), it can be seen that ATS-1 and ATS-2, which are located at the north side of the building, experienced the highest uplift force because the WSPs were parallel to the motion of the shake table and also had to resist to additional lateral force due to the torsional response of the building. The ATS rods installed at the end posts of WSP-D (ATS-5 and ATS-6) experienced the second largest uplift force because the WSP located at line D was also parallel to the motion of the shake table.

Table 3. Maximum Uplift Forces during Cape Mendocino-Rio Ground Motion Scaled to $S_a = 1.8$ g

		ATS uplift force (kN)[a]							
	Story	WSP-A		WSP-3R		WSP-D		WSP-3	
Phase	number	ATS-1	ATS-2	ATS-3	ATS-4	ATS-5	ATS-6	ATS-7	ATS-8
PBSR	4	16.1	14.7	2.4	4.3	11.5	9.4	1.8	1.1
SMF	3	31.5	26.6	3.9	4.8	26.1	31.5	1.3	3.8
	2	52.8	62.6	7.9	12.1	53.8	38.1	7.3	7.8
	1	85.5	99.4	7.9	11.0	—[b]	—[b]	4.3	3.7
PBSR	4	1.9	0.7	8.1	33.7	2.6	2.7	7.2	2.7
FVD	3	1.3	1.7	56.6	59.9	5.6	3.6	21.2	20.7
	2	1.9	2.8	73.8	90.4	12.3	13.6	31.8	33.3
	1	55.2	67.9	6.8	6.7	—[b]	—[b]	0.0	0.0

[a]1 kip = 4.448 kN.
[b]ATS-5 and ATS-6 were attached to the steel frame in the first story to avoid interference with the garage space.

In the fourth phase of testing (i.e., PBSR FVD), the maximum uplift force occurred in ATS-3 and ATS-4, which were installed at the WSP-3R perpendicular to the direction of motion of the shake table. This was due to the fact that the response of the WSP to the

Downloaded from ascelibrary.org by University of Wisconsin-Madison on 10/03/17. Copyright ASCE. For personal use only; all rights reserved.

Fig. 19. Typical damage observed in (a) P-807 SMF retrofits at first story; (b) P-807 SMF retrofits at second story; (c) PBSR SMF at the first story; (d) PBSR SMF at the third story

lateral load induced by ground excitation is likely out of phase with the response of the damper frame (i.e., FVDs); therefore, the WSPs had to carry almost all the lateral force at the maximum lateral displacement of the building at the point in time the dampers were carrying almost zero force (due to zero velocity at maximum displacement). This fact is also true for resisting torsional moments. Because WSP-3R had to resist against lateral force and torsional moment, the ATS rods associated with the shear wall (i.e., ATS-3 and ATS-4) experienced largest uplift force. The second highest uplift forces were recorded at the ATS rods located at the end posts of WSP-A.

Damage Inspection

A thorough damage inspection was conducted after each seismic test to evaluate what, if any, structural and nonstructural damage occurred during each test. Fig. 19 presents photos of typical damage that occurred during Phases 2 and 3. These two phases were selected because in both of them the SMF was used to retrofit the building but one design was based on FEMA P-807 and the other was based on the PBSR methodology. Figs. 19(a and b) show damage that occurred during the Loma Prieta ground motion for the walls in the X-direction at the first story and the second story, respectively. Significant damage can be seen at the first story (laundry room) but only a very small crack (hairline) was observed next to the corner of a window at the second story. This confirms that for the FEMA P-807 retrofit methodology, the first story is expected to experience significant damage while the upper stories do not experience significant damage because of their box-like rigid-body behavior during excitation.

As mentioned previously, for the PBSR methodology it is expected that all stories will experience similar drifts. Figs. 19(c and d) present damage that occurred in the first story (laundry room) and in the third story, respectively, during the last two MCE-level tests. Diagonal cracks on the drywall at the corner of the window of the laundry room and cracks in WSPs and partial nail withdrawal were observed after the building was subjected to MCE-level ground motions. However, it is important to recall that the level of shaking for the PBSR test results shown in these pictures is at the MCE level, while the FEMA P-807 results shown previously are at 1.1 g, i.e., slightly less than the design basis earthquake (DBE) level.

Summary and Conclusions

A full-scale four-story wood-frame building with a soft story at its first floor was retrofitted using two different retrofit methodologies and four different retrofit techniques. FEMA P-807 and PBSR methodologies were used to design the retrofits. CLT rocking walls, steel SMFs, WSPs, and FVDs were used as retrofit techniques. The building was subjected to the Loma Prieta-Gilroy and Cape Mendocino-Rio earthquake records scaled to spectral accelerations ranging from 0.2 to 1.8 g. The observed behavior of the retrofitted building was close to the design criteria for each test. In the FEMA P-807-based retrofits, the maximum interstory drift was observed at the first story and much less damage was transferred to the upper stories, whereas in the PBSR retrofits, damage was distributed over the height of the building, which helped the building resist ground excitations with much higher intensities by distributing seismic demand over the height of the building. The translational response of the building at each story was close to the target performance criteria used in the design for both FEMA P-807 and PBSR retrofit procedures. The torsional response of the building was minor as compared with the translational response, which confirms that the building was retrofitted such that the eccentricities at the stories were small following retrofits. It can be concluded that (1) a retrofit in accordance with the FEMA P-807 guidelines (retrofit limited to the first story) is suitable for achieving a life safety performance level during strong earthquakes when retrofit of all story levels is

Downloaded from ascelibrary.org by University of Wisconsin-Madison on 10/03/17. Copyright ASCE. For personal use only; all rights reserved.

not possible due to one or more constraints, and (2) the PBSR methodology can be applied to soft-story wood-frame buildings and promotes a relatively uniform distribution of seismic demand over the height of the structure, thereby allowing the building to resist very large earthquakes with a very low probability of collapse.

Acknowledgments

This material is based on work supported by the National Science Foundation under Grant No. CMMI-1041631 and 1314957 (NEES Research) and NEES Operations. Any opinions, findings, and conclusions or recommendations expressed in this material are those of the investigators and do not necessarily reflect the views of the National Science Foundation. A sincere thank you to Simpson Strong Tie for their financial, personnel, and product support throughout the project, including the engineering support for the SMF in San Diego. Cash, personnel, or in-kind contributions were provided by the USDA Forest Products Laboratory, Structural Engineers Association of Southern California, Taylor Devices, and Innovative Timber Solutions/Smartwood. The authors kindly acknowledge the other co-principal investigators (Co-PI's) of the project, Weichiang Pang and Xiaoyun Shao, and other senior personnel of the NEES-Soft project: David V. Rosowsky at University of Vermont, Andre Filiatrault at University at Buffalo, Shiling Pei at South Dakota State University, David Mar at Tipping Mar, and Charles Chadwell at Cal-Poly San Luis Obispo; the other graduate students participating on the project: Ph.D. student Ershad Ziaei (Clemson University) and M.Sc. students Jason Au and Robert McDougal at Cal-Poly Pomona; and the practitioner advisory committee: Laurence Kornfield, Tom Van Dorpe, Doug Thompson, Kelly Cobeen, Janiele Maffei, Douglas Taylor, and Rose Grant. A special thank you to all of the research experience for undergraduate (REU) students: Sandra Gutierrez, Faith Silva, Gabriel Banuelos, Rocky Chen, and Connie Tsui. Others that have helped include Asif Iqbal, Andre Barbosa, Vaishak Gopi, Steve Yang, Ed Santos, Tim Ellis, Omar Amini, Russell Ek, Rakesh Gupta, and Anthonie Kramer. Finally, our sincere thank you to NEES and all site staff and site principal investigator (PI's) at NEES at UCSD for their assistance in getting the test specimen ready for testing and in conducting the tests.

References

ASCE. (2010). "Minimum design loads for buildings and other structures." *ASCE/SEI 7-10*, Reston, VA.

Bahmani, P., van de Lindt, J. W., Gershfeld, M., Mochizuki, G. L., Pryor, S. E., and Rammer, D. (2014). "Experimental seismic behavior of a full-scale four-story soft-story woodframe building with retrofits I: building design, retrofit methodology, and numerical validation." *J. Struct. Eng.*, in press.

Chopra, A. K. (2005). *Dynamics of structures: Theory and applications to earthquake engineering*, 5th Ed., Prentice Hall, Upper Saddle River, NJ.

FEMA (Federal Emergency Management Agency). (2009). "Quantification of building seismic performance factors." *FEMA P-695*, Washington, DC.

FEMA (Federal Emergency Management Agency). (2012). "Seismic evaluation and retrofit of multi-unit wood-frame buildings with weak first stories." *FEMA P-807*, Washington, DC.

Karacabeyli, E., and Douglas, B., ed. (2013). *CLT Handbook*, U.S. Edition, FPInnovations, Pointe-Claire, QC, Canada.

Ozcelik, O., Luco, J. E., Conte, J. P., Trombetti, T. L., and Restrepo, J. I. (2008). "Experimental characterization, modeling and identification of the NEES-UCSD shake table mechanical system." *Earthquake Eng. Struct. Dyn.*, 37(2), 243–264.

Schott, F. H., Lee, D. A., Karns, J., and Symans, M. D. (2014). "Sustainability in soft weak open front buildings." *Proc., 10th National Conf. on Earthquake Engineering (10NCEE)*, Earthquake Engineering Research Institute (EERI), Oakland, CA.

Tian, J., and Symans, M. D. (2012). "Strategic plan-wise distribution of damping devices for seismic protection of soft-story buildings." *Proc., 1st Int. Conf. on Performance-Based and Life-Cycle Structural Engineering*, Hong Kong Polytechnic Univ., Hong Kong, China.

Tian, J., Symans, M. D., Gershfeld, M., Bahmani, P., and van de Lindt, J. W. (2014). "Seismic performance of a full-scale soft-story woodframed building with energy dissipation retrofit." *Proc., 10th National Conf. on Earthquake Engineering (10NCEE)*, Earthquake Engineering Research Institute (EERI), Oakland, CA.

Downloaded from ascelibrary.org by University of Wisconsin-Madison on 10/03/17. Copyright ASCE. For personal use only; all rights reserved.